ISSN 1674-1056
http://cpb.iphy.ac.cn
http://iopscience.iop.org/cpb
中国物理 B
Chinese Physics
中国物理 Chinese Physics B

Nuclear magnetic resonance measurement station in SECUF using hybrid superconducting magnets

Zheng Li(李政), Guo-qing Zheng(郑国庆)

Citation: Chin. Phys. B . 2018, 27(7): 077404. **doi:** 10.1088/1674-1056/27/7/077404

Journal homepage: http://cpb.iphy.ac.cn; http://iopscience.iop.org/cpb

What follows is a list of articles you may be interested in

Structural phase transition, precursory electronic anomaly, and strong-coupling superconductivity in quasi-skutterudite $(Sr_{1-x}Ca_x)_3Ir_4Sn_{13}$ and $Ca_3Rh_4Sn_{13}$

Jun Luo(罗军), Jie Yang(杨杰), S Maeda, Zheng Li(李政), Guo-Qing Zheng(郑国庆)
Chin. Phys. B . 2018, 27(7): 077401. **doi:** 10.1088/1674-1056/27/7/077401

Parallel variable-density spiral imaging using nonlocal total variation reconstruction

Fang Sheng, Guo Hua
Chin. Phys. B . 2014, 23(5): 057401. **doi:** 10.1088/1674-1056/23/5/057401

Review of nuclear magnetic resonance studies on iron-based superconductors

Ma Long, Yu Wei-Qiang
Chin. Phys. B . 2013, 22(8): 087414. **doi:** 10.1088/1674-1056/22/8/087414

Quenched Fe moment in the collapsed tetragonal phase of $Ca_{1-x}Pr_xFe_2As_2$

Ma Long, Gi Gao-Feng, Dai Jia, Saha S R, Drye T, Paglione J, Yu Wei-Qiang
Chin. Phys. B . 2013, 22(5): 057401. **doi:** 10.1088/1674-1056/22/5/057401

Study on signal intensity of low field nuclear magnetic resonance via indirect coupling measurement

Jiang Feng-Ying, Wang Ning, Jin Yi-Rong, Deng Hui, Tian Ye, Lang Pei-Lin, Li Jie, Chen Ying-Fei, Zheng Dong-Ning
Chin. Phys. B . 2013, 22(4): 047401. **doi:** 10.1088/1674-1056/22/4/047401

TOPICAL REVIEW — Synergetic Extreme Condition User Facility: Breakthroughs and opportunities for the research of physical science

Nuclear magnetic resonance measurement station in SECUF using hybrid superconducting magnets*

Zheng Li(李政)[1,2,†] and Guo-qing Zheng(郑国庆)[1,2,‡]

[1] *Beijing National Laboratory for Condensed Matter Physics, Institute of Physics, Chinese Academy of Sciences, Beijing* 100190, *China*
[2] *School of Physical Sciences, University of Chinese Academy of Sciences, Beijing* 100190, *China*

(Received 25 April 2018; revised manuscript received 19 May 2018; published online 1 June 2018)

Nuclear magnetic resonance (NMR) is one of the most powerful tools to explore new quantum states of condensed matter induced by high magnetic fields at a microscopic level. High magnetic field enhances the intensity of the NMR signal, and more importantly, can induce novel phenomena. In this article, examples are given on the field-induced charge density wave (CDW) in high-T_c superconductors and on the studies of quantum spin liquids. We provide a brief introduction to the high magnetic field NMR platform, the station 4 of the Synergetic Extreme Condition User Facility (SECUF), being built at Huairou, Beijing.

Keywords: nuclear magnetic resonance (NMR), high magnetic field, charge density wave (CDW)

PACS: 74.25.nj, 76.60.–k, 71.45.Lr, 74.25.Dw **DOI:** 10.1088/1674-1056/27/7/077404

1. Introduction

Nuclear magnetic resonance (NMR) is widely used to characterize the properties of new materials in physics, chemistry, and biology. The most important requirements of the NMR technique are magnets with high field strength B_0, high homogeneity, and high stability. Large B_0 is essential to boost the NMR signal intensity, which is proportional to B_0^2. Currently, a field of 23.5 T is available for the NMR superconducting magnet made of Sb_3Sn wire operating at 1.9 K,[1] which is the limit of the obtainable field strengths of low temperature superconductors (LTS). Recent breakthrough has been made to use new high-temperature superconductors (HTS). A hybrid LTS/HTS superconducting magnet with cold bore size of 34 mm was implented at National High Magnetic Field Laboratory (NHMFL), Tallahassee in 2017, which produces a field of 32 T with homogeneity about 500 ppm/cm^3 for general purpose.[2] A hybrid LTS/HTS magnet for NMR is being built at Synergetic Extreme Condition User Facility (SECUF) at Huairou, Beijing, thereby enabling new applications at the forefront of modern multidisciplinary research.

Magnetic fields can suppress superconducting (SC) transition temperature T_c, and reveal novel states hidden below T_c. For example, NMR study on cuprate high-T_c superconductors $Bi_2Sr_{2-x}La_xCuO_{6+\delta}$ (Bi2201) shows that when the superconductivity is completely suppressed, a metallic pseudogap state appears as the ground state.[3,4] When a high magnetic field (HMF) is applied perpendicular to the CuO_2 plane of $YBa_2Cu_3O_{7-y}$ (YBCO), charge density wave (CDW) is found below the superconducting dome.[5] Recently, ^{63}Cu-NMR measurement on single-layered $Bi_2Sr_{2-x}La_xCuO_6$ discovered a long-range CDW induced by an in-plane field, setting in even far above the superconducting dome.[6] Magnetic field is also an important parameter in the studies of quantum spin liquids.[7,8]

2. Example 1: high magnetic field NMR on cuprate high-T_c superconductors

High-T_c superconductivity is obtained by doping a Mott insulator,[9] and the spin interaction is believed to be important for the superconductivity.[10] However, the electron pairing mechanism is still elusive, largely because the normal-state properties are not well understood.[11,12] For example, at low carrier concentration region p ($0 < p < 0.2$), there appears a pseudogap, where partial density of states (DOS) is suppressed below a characteristic temperature T^* well above T_c.[13] Application of a high magnetic field is useful to study the ground state properties of the pseudogap and to diagnose the interplay between various orders in the cuprates.

NMR measurements on $Bi_2Sr_{2-x}La_xCuO_{6+\delta}$ carried out under high magnetic fields revealed the complete phase diagram. When superconductivity is suppressed completely, the pseudogap ground state is revealed. As shown in Fig. 1, the

*Project supported by the Strategic Priority Research Program of the Chinese Academy of Sciences (Grant No. XDB07020200), the National Key Research and Development Program of China (Grant Nos. 2016YFA0300502 and 2015CB921304), and the National Natural Science Foundation of China (Grant No. 11634015).

†Corresponding author. E-mail: lizheng@iphy.ac.cn
‡Corresponding author. E-mail: gqzheng@iphy.ac.cn

© 2018 Chinese Physical Society and IOP Publishing Ltd

pseudogap ground state is a metallic state with a finite DOS which decreases with decreasing doping but remains quite large even at the vicinity of the magnetically ordered phase.

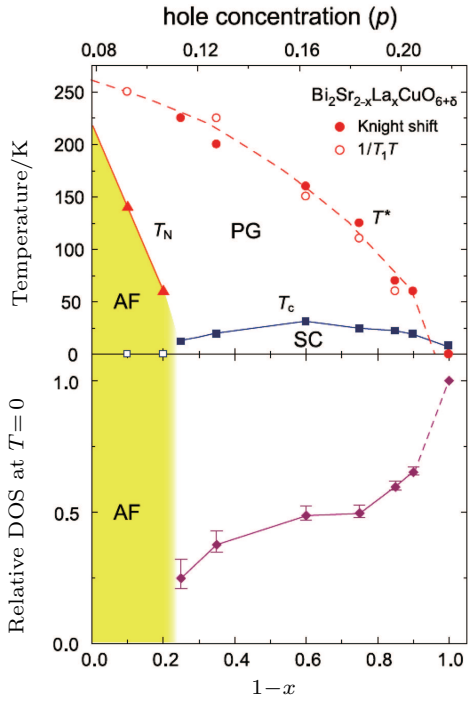


Fig. 1. (color online) Phase diagram of $Bi_2Sr_{2-x}La_xCuO_{6+\delta}$. The upper panel shows characteristic temperatures vs $1-x$ ($\propto$ hole concentration). The lower panel shows the hole-concentration dependence of relative DOS at $T=0$.

In YBCO, when superconductivity is suppressed, ^{63}Cu NMR at $H = 28.5$ T revealed a long-range charge density modulation perpendicular to the CuO-chain in the sample with $p = 0.108$.[14] Resonant elastic and inelastic x-ray spectroscopy also indicated that a high field induces a correlation along the CuO-chain direction and modifies the coupling between the CuO_2 bilayers, thus causing a three-dimensional CDW.[15,16] These observations are consistent with early discovery of a Fermi-surface reconstruction by quantum oscillations.[17] As the long-range CDW onsets below $T_c(H=0)$ and only emerges when the field is applied perpendicular to the CuO_2 plane, a widespread speculation is that it is due to incipient CDW in the vortex cores[18] that becomes overlapped as the field becomes stronger.[19–21] In fact, a field as large as 28.5 T applied in the CuO_2-plane of YBCO did not bring about any long-range CDW.[14]

Recently, a breakthrough for this issue was made by high magnetic field NMR on Bi2201. A high magnetic field parallel to the Cu–O bond direction ($H \parallel a$ or b axis) in Bi2201, which does not create vortex cores in the CuO_2 plane, induced a CDW order above the superconducting dome,[6] in contrast to that in YBCO where CDW appears below $T_c(H=0)$.[14,21] As shown in Fig. 2, the H_{CDW} is slightly lower than that in YBCO, suggesting that CDW has a similar energy scale across different classes of cuprates. However, the relationship between H_{CDW} and H_{c2} is completely different from that seen in YBCO where H_{CDW} is scaled with H_{c2}. In Bi2201, H_{CDW} and T_{CDW} are more related with doping, rather than with H_{c2}. The long-range CDW order is induced more easily closer to the AF phase boundary. Figure 3 compares the phase diagram of Bi2201 with that of YBCO. For Bi2201, the CDW order becomes the successor of the AF order beyond $p = 0.107$ at which superconductivity starts to emerge.

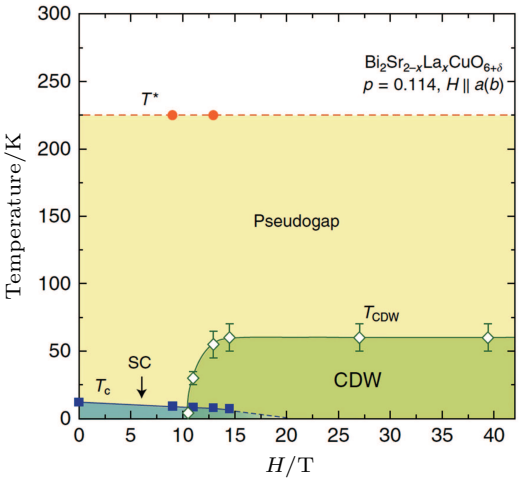


Fig. 2. (color online) H–T phase diagram for underdoped Bi2201. The T^* is the pseudogap temperature.

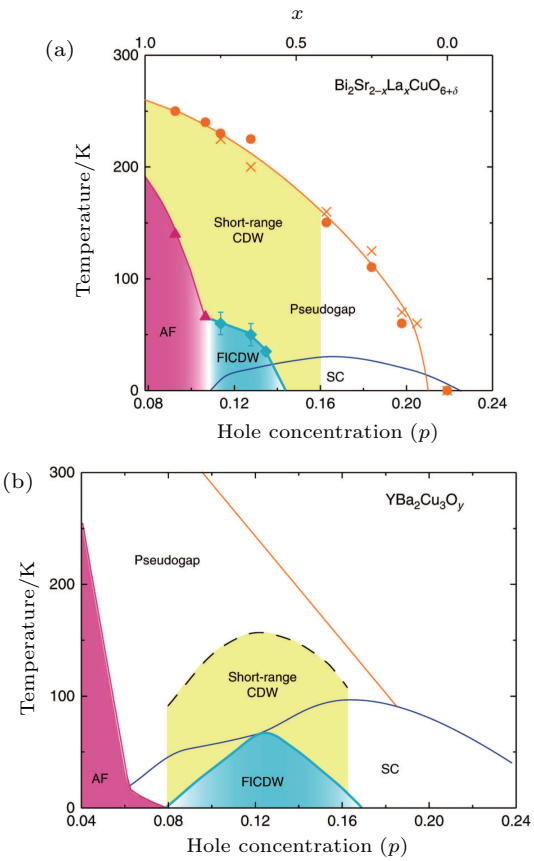


Fig. 3. (color online) Phase diagram of Bi2201 compared with that of YBCO. Doping dependence of the short-range CDW reported by the x-ray measurements[11,22,23] and the field-induced CDW (FICDW) for Bi2201 (a) and YBCO (b). For both cases, T_c is the zero-field value. Error bars represent the uncertainty in defining T_{CDW}.

The phase diagram shown in Fig. 4 reveals several important things. First and most remarkably, down-shifting the T^* curve in temperature coincides with the T_{CDW} curve, which may suggest that the pseudogap is a fluctuating form of the long-range order. Second, the T_{CDW} takes over T_N when superconductivity emerges, but disappears well before the pseudogap closes. This points to the important role of charge degree of freedom in high-temperature superconductivity.

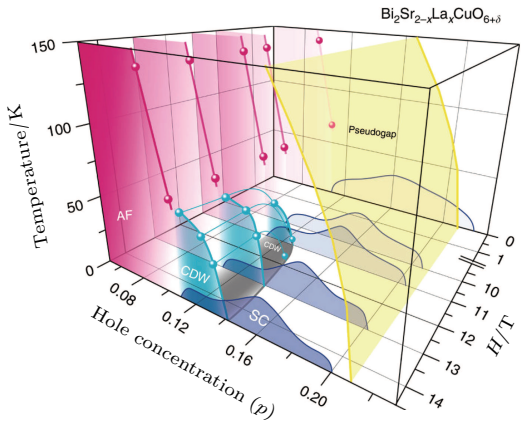


Fig. 4. (color online) Magnetic-field evolution of the phase diagram. Hole concentration (p) dependence of the pseudogap temperature T^*, T_N, and T_c, and the p- and H-dependence of T_{CDW} for $Bi_2Sr_{2-x}La_xCuO_{6+\delta}$. Magnetic field is applied along the Cu–O bond direction ($H \parallel a(b)$).

3. Example 2: using high magnetic field to characterize the topological properties of the quantum spin liquids

A quantum spin liquid (QSL) is a system with magnetic interaction among spins but has no long range magnetic order down to zero temperature. It is characterized by the pattern of long-range quantum entanglement that has no classical counterpart. It was proposed as a mechanism for high-temperature superconductivity[24] and as a material system for topological quantum computation.[25] The pursuit of QSL has a long history. We introduce two examples in which the magnetic field has played an important role in establishing the QSL states and in characterizing the properties of the new states.

Zn doped barlowite $Cu_3Zn(OH)_6FBr$ with a Kagome lattice (Fig. 5(a)) was recently successfully synthesized.[7] It has minimum disorder and small Dzyaloshinsky–Moriya interaction, which are important to realize a QSL state. No magnetic order was found down to 50 mK. The spin susceptibility measured by ^{19}F NMR goes away completely at the zero-temperature limit, which indicates a gapped QSL state.[7] Moreover, the magnetic field dependence of the spin susceptibility reveals a spin $1/2$ excitation, as shown in Fig. 5(b). This is an important insight showing that the spin excitation of the QSL state in $Cu_3Zn(OH)_6FBr$ is spinon. Namely, the excitation is fractionalized, in close similarity to the charge fractionalization of fractional quantum Hall systems.

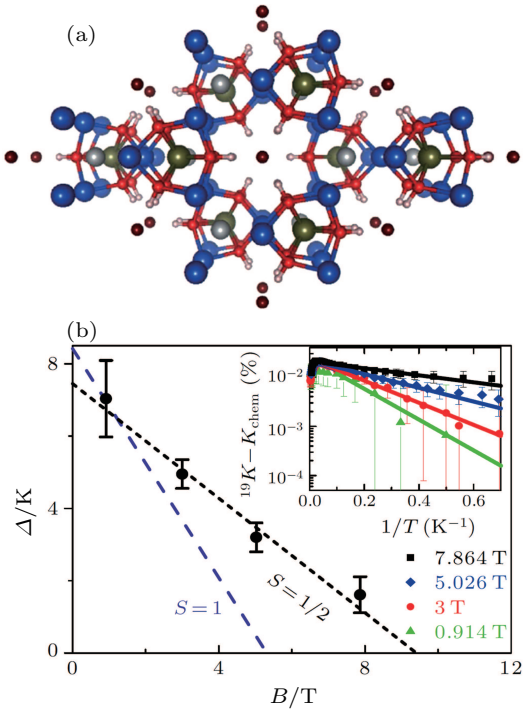


Fig. 5. (color online) (a) Top view of the $Cu_3Zn(OH)_6FBr$ crystal structure, where F (brown) is in the center between two hexagons of two kagome Cu planes. (b) Magnetic field dependence of the spin gap. The black short-dash line is fitted by $\Delta(B) = \Delta(0) - g\mu_B SB$ with spin quantum number $S = 1/2$, where g-factor obtained from bulk magnetic susceptibility is $g = 2.4$ and μ_B is the Bohr magneton. For comparison, $\Delta(B)$ for $S = 1$ is shown by the blue dash line constrained by the value at 0.914 T, which hardly describes the data. Inset shows the Arrhenius plot of $^{19}K - K_{chem}$ with the vertical axis in logarithmic scale, which demonstrates visually that the gap decreases with increasing magnetic field. The solid curve is the fitting function $A\exp(-\Delta/T)$ for $^{19}K - K_{chem}$.[7]

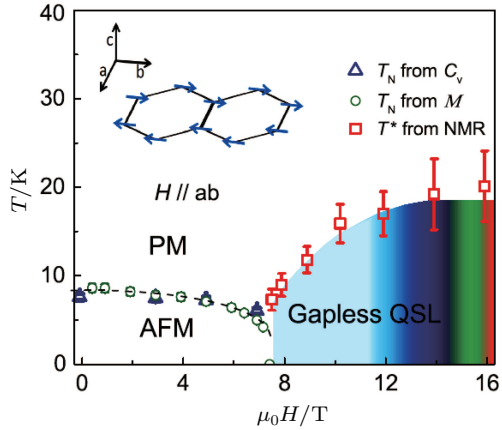


Fig. 6. (color online) Magnetic phase diagram of α-$RuCl_3$ with field applied in the ab plane. T_N is determined from magnetization and specific-heat data. T^* represents the upper limit of the gapless low-T regime. Inset: schematic representation of zero-field zigzag order in the hexagonal (ab) plane.[8]

The compound α-$RuCl_3$ has a honeycomb lattice and bond-directional Ising-type interactions on the three distinct links. Unfortunately, this system undergoes a phase transition to a magnetically ordered state at $T = 8$ K. However, recent ^{35}Cl NMR measurements suggested that a magnetic field about 8 T can suppress such long-range ordered state and induces a gapless QSL state (Fig. 6).[8] This work is another

good example that the magnetic field can be used to obtain new quantum states.

4. NMR station in SECUF

Although high magnetic field NMR can be performed at several facilities in the world with magnet field up to 45 T using resistive or SC/resistive hybrid magnets, the running cost is huge. For example, a huge power of about 30 MW is consumed at 45 T, which limits the experimental time. The sample size is also limited due to insufficient homogeneity. China is presently developing the high magnetic field technique and has built a hybrid magnet at 40 T,[26] which promotes frontier researches on condensed matter physics, material science, chemistry, and life science. Meanwhile, China is also building hybrid superconducting high field magnets for special applications. A high magnetic field NMR platform as the station 4 of SECUF and also a quantum oscillation measurement platform as the station 2 of SECUF will be built at Huairou, Beijing. The high-magnetic-field laboratories around the globe and the parameters of some of their magnets are listed in Table 1.

Table 1. High-magnetic-field laboratories around the globe. SC stands for superconducting.

Laboratory	Location	Field/T	Type	Bore size/mm	Homogeneity/ppm·cm^{-3}	Power/MW
Preparation for the station 4 of SECUF	Beijing, China	25	all SC	50	10	
National High Magnetic Field Laboratory	Tallahassee, USA	45	SC/resistive	32	300	30
		36	SC/resistive	40	1	14
		32	all SC	34	500	
Chinese High Magnetic Field Laboratory	Hefei, China	40	SC/resistive	32	130	28
Laboratoire National des Champs Magnetiques Intenses	Grenoble, France	35	SC/resistive	34	700	24
High Field Magnet Laboratory	Nijmegen, Netherlands	37.9	SC/resistive	32	1000	20
High Field Laboratory for Superconducting Materials	Sendai, Japan	24.6	all SC	52	>100	

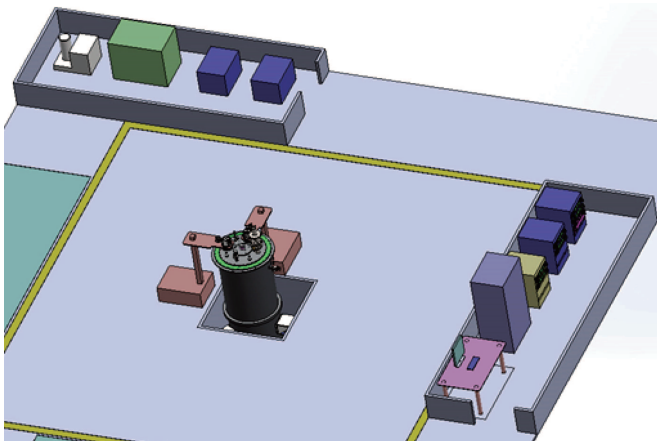


Fig. 7. (color online) Schematic view of the HMF NMR system with a hybrid LTS/HTS magnet.

The high magnetic field NMR platform will integrate a solid-state NMR spectrometer with a domestic-made 25 T superconducting magnet which consists of a conventional low-temperature and a novel high-temperature superconductor. The high-temperature superconducting magnet, which has low running cost and provides unlimited duration of the experiments, will be built by Institute of Electric Engineering (IEE), CAS. It will have a homogeneity of 10 ppm/cm^3 and a stability of 10 ppm/h, which are satisfactory for solid-state NMR. The cold bore with the size of 50 mm is capable for a cryostat with large sample space to accommodate components such as pressure cell, sample rotator, and so on. A dilution refrigerator will be installed to probe microscopic properties of matter down to 20 mK. NMR spectrometers and probes with auto-tuning capability over a frequency range of 1 MHz to 400 MHz are being built. Figure 7 shows the schematic view of the HMF NMR subsystem platform. It will work as a research facility available both to internal researchers of SECUF as well as to external users. The emphasis is put on the user-friendly design in terms of both hardware and software. The low running cost and high stability of the all-superconducting magnet will provide a stable and reliable platform for high-field NMR researches. Combining with high pressure and ultra-low temperature environments, this platform is expected to better serve the community to explore quantum phase transition, mechanism for high temperature superconductivity, topological quantum materials, and so on.

References

[1] Bhattacharya A 2010 *Nature* **463** 605
[2] https://nationalmaglab.org/news-events/news/new-world-record-magnet-fulfills-superconducting-promise
[3] Zheng G Q, Kuhns P L, Reyes A P, Liang B and Lin C T 2005 *Phys. Rev. Lett.* **94** 047006
[4] Kawasaki S, Lin C T, Kuhns P L, Reyes A P and Zheng G Q 2010 *Phys. Rev. Lett.* **105** 137002
[5] Wu T, Mayaffre H, Kramer S, Horvatic M, Berthier C, Hardy W N, Liang R X, Bonn D A and Julien M H 2015 *Nat. Commun.* **6** 6438
[6] Kawasaki S, Li Z, Kitahashi M, Lin C T, Kuhns P L, Reyes A P and Zheng G Q 2017 *Nat. Commun.* **8** 1267
[7] Feng Z, Li Z, Meng X, Yi W, Wei Y, Zhang J, Wang Y-C, Jiang W, Liu Z, Li S, Liu F, Luo J, Li S, Zheng G Q, Meng Z Y, Mei J W and Shi Y 2017 *Chin. Phys. Lett.* **34** 077502
[8] Zheng J, Ran K, Li T, Wang J, Wang P, Liu B, Liu Z X, Normand B, Wen J and Yu W 2017 *Phys. Rev. Lett.* **119** 227208
[9] Bednorz J G and Müller K A 1986 *Zeitschrift für Physik B Condensed Matter* **64** 189
[10] Lee P A, Nagaosa N and Wen X G 2006 *Rev. Mod. Phys.* **78** 17
[11] Keimer B, Kivelson S A, Norman M R, Uchida S and Zaanen J 2015 *Nature* **518** 179
[12] Fradkin E, Kivelson S A and Tranquada J M 2015 *Rev. Mod. Phys.* **87** 457
[13] Timusk T and Statt B 1999 *Rep. Prog. Phys.* **62** 61

[14] Wu T, Mayaffre H, Kramer S, Horvatic M, Berthier C, Hardy W N, Liang R X, Bonn D A and Julien M H 2011 *Nature* **477** 191
[15] Gerber S, Jang H, Nojiri H, Matsuzawa S, Yasumura H, Bonn D A, Liang R, Hardy W N, Islam Z, Mehta A, Song S, Sikorski M, Stefanescu D, Feng Y, Kivelson S A, Devereaux T P, Shen Z X, Kao C C, Lee W S, Zhu D and Lee J S 2015 *Science* **350** 949
[16] Chang J, Blackburn E, Ivashko O, Holmes A T, Christensen N B, Hucker M, Liang R, Bonn D A, Hardy W N, Rutt U, Zimmermann M, Forgan E M and Hayden S M 2016 *Nat. Commun.* **7** 11494
[17] Doiron-Leyraud N, Proust C, LeBoeuf D, Levallois J, Bonnemaison J B, Liang R X, Bonn D A, Hardy W N and Taillefer L 2007 *Nature* **447** 565
[18] Hoffman J E, Hudson E W, Lang K M, Madhavan V, Eisaki H, Uchida S and Davis J C 2002 *Science* **295** 466
[19] Chang J, Doiron-Leyraud N, Cyr-Choiniere O, Grissonnanche G, Laliberte F, Hassinger E, Reid J P, Daou R, Pyon S, Takayama T, Takagi H and Taillefer L 2012 *Nat. Phys.* **8** 751
[20] Neto E H D, Aynajian P, Frano A, Comin R, Schierle E, Weschke E, Gyenis A, Wen J S, Schneeloch J, Xu Z J, Ono S, Gu G D, Le Tacon M and Yazdani A 2014 *Science* **343** 393
[21] Wu T, Mayaffre H, Kramer S, Horvatic M, Berthier C, Kuhns P L, Reyes A P, Liang R X, Hardy W N, Bonn D A and Julien M H 2013 *Nat. Commun.* **4** 2113
[22] Comin R, Frano A, Yee M M, Yoshida Y, Eisaki H, Schierle E, Weschke E, Sutarto R, He F, Soumyanarayanan A, He Y, Le Tacon M, Elfimov I S, Hoffman J E, Sawatzky G A, Keimer B and Damascelli A 2014 *Science* **343** 390
[23] Peng Y Y, Salluzzo M, Sun X, Ponti A, Betto D, Ferretti A M, Fumagalli F, Kummer K, Le Tacon M, Zhou X J, Brookes N B, Braicovich L and Ghiringhelli G 2016 *Phys. Rev. B* **94** 184511
[24] Anderson P W 1987 *Science* **235** 1196
[25] Kitaev A Y 2003 *Ann. Phys.* **303** 2
[26] http://english.hmfl.cas.cn/news/news_archive/2017/201709/t20170929_183607.html